Chemical Science

Accepted Manuscript

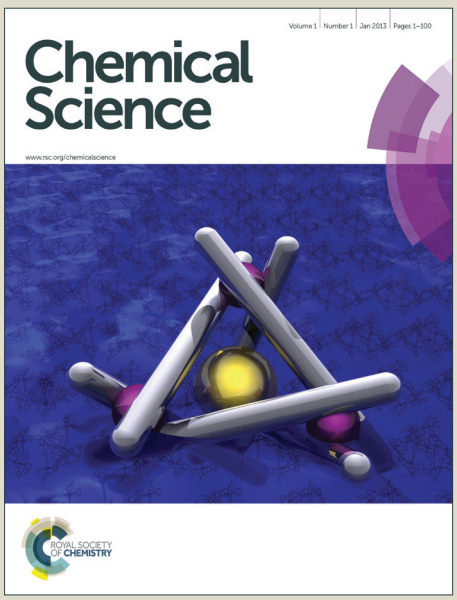

ROYAL SOCIETY OF CHEMISTRY

www.rsc.org/chemicalscience

Journal Name

RSCPublishing

PERSPECTIVE

$[M_3(\mu_3\text{-}O)(O_2CR)_6]$ and Related Trigonal Prisms: Versatile Molecular Building Blocks for Crystal Engineering of Metal-Organic Material Platforms.

Cite this: DOI: 10.1039/x0xx00000x

Received ooth January 2012,
Accepted ooth January 2012

DOI: 10.1039/x0xx00000x

www.rsc.org/

Alexander Schoedel[a] and Michael J. Zaworotko[a,b]

This review details the emergence of metal-organic materials (MOMs) sustained by high symmetry trigonal prismatic molecular building blocks (MBBs). MOMs have attracted general attention over the past two decades as judicious selection of MBBs allows crystal engineers to exert exquisite control over MOM structure, which, when combined with their modularity, diverse composition and fine-tuneable structural features, makes their properties controllable in a manner uncommon in materials science. In this context, tetrahedral and octahedral MBBs, which readily afford diamondoid (**dia**) or primitive cubic (**pcu**) nets, respectively, are the most commonly studied MBBs. However, trigonal prismatic MBBs have also captured the imagination of crystal engineers since they can sustain stable, high symmetry, extra-large surface area nets with new topologies and exhibit excellent gas sorption performance. Nets formed by linking $[M_3(\mu_3\text{-}O)(O_2CR)_6]$ MBBs are of particular interest and are discussed from a crystal engineering perspective. These MBBs can form discrete (0-D) polyhedra, 2-D grids and 3-D nets that represent families or "platforms" that enable systematic studies of structure/property relationships. The development of decorated $[M_3(\mu_3\text{-}O)(O_2CR)_6]$ MBBs that facilitate a 2-step strategy for generation of novel MOM platforms from simple, low cost MBBs, is also discussed.

Introduction

Metal-Organic Materials (MOMs) have been intensively studied over the past two decades thanks to their many potential applications.[1,2,3] MOMs are typically assembled from metal ions or clusters (nodes) and organic multifunctional ligands (linkers) to afford periodic networks that contain channels and cavities with controllable size and chemistry.[4] In contrast to other classes of porous materials (e.g. zeolites)[5], the modular nature of MOMs and their amenability to fine-tuning of properties has enabled their development as materials for gas purification and storage[6], catalysis,[7] small-molecule separation[8] and chemical sensing.[9]

MOMs gained particular traction when the concept of crystal engineering was popularized in the early 1990's.[10] The definition of crystal engineering was coined more than 25 years ago[6] yet it is still relevant today. Simply put, crystal engineering, the design and synthesis of functional materials with desired properties, provided early rationale for development of MOMs, especially in the context of high symmetry nets generated by direct linking of polyhedral or polygonal nodes. Such nodes offer different connectivity (from 3-connected upwards) and, when propagated by linear linkers according to the "node and spacer" principle,[11] often result in nets with predictable topology and structure.

Alexander Schoedel was born in Munich, Germany. He obtained his Diploma degree (equiv. M.Sc.) in chemistry from the Ludwig Maximilians University Munich under the supervision of Professor Thomas Bein. He then joined Professor Michael J. Zaworotko's research group at the University of South Florida (USF) in 2010 and has since been working towards completion of a PhD degree in inorganic chemistry. His current research interests encompass crystal engineering, metal-organic materials, supramolecular chemistry, and topological crystal chemistry as well as gas storage and separation applications.

Dr. Mike Zaworotko currently serves as Bernal Chair of Crystal Engineering and Science Foundation of Ireland Research Professor at the University of Limerick, Ireland. He was born in Wales in 1956 and received his B.Sc. and Ph.D. degrees from Imperial College (1977) and the University of Alabama (1982), respectively. He served as a faculty member at Saint Mary's University, Nova Scotia, Canada, from 1985-1998, at University of Winnipeg, Canada from 1998-99 and at the University of South Florida, USA, from 1999-2013. Research interests have focused upon fundamental and applied aspects of crystal engineering since 1990.

The resulting networks can then be described in terms of their network topology which is principally related to coordination environment of the node or Molecular Building Block (MBB).[12] Herein, high symmetry trigonal prismatic MBBs are highlighted together with the related vertex figures that sustain the resulting topologies.

High Symmetry Molecular Building Blocks (MBBs)

First generation MOMs are exemplified by single metal ion nodes linked by pyridyl linkers, e.g. 4,4'-bipyridine. The resulting networks are controlled by the coordination geometry of the metal ions. Prototypal topologies such as **dia**[13,14], **sql**[15] or **pcu**[16], all of which can exhibit the phenomenon of interpenetration,[2,17,18] were thereby introduced. The second generation of MOMs are exemplified by high-symmetry metal-carboxylate cluster MBBs and proved generally more robust, allowing for the removal of guest species from the cavities or channels of the framework. Many of the resulting MOMs were found to be permanently porous and the greater relative size of their MBBs compared to first generation MOMs resulted in extra-large surface areas and pore sizes. From a crystal engineering perspective, high symmetry MBBs enable exquisite control over the coordination environment, which makes them highly desirable for the rational design of new networks. The level of interest in MOMs increased exponentially after the pioneering work of Williams,[19] Yaghi[20] and Kitagawa[21] with respect to permanent porosity. Yaghi and Kitagawa coined the terms metal-organic frameworks (MOFs) and porous coordination polymers (PCPs), respectively. The large number of MOMs that have subsequently been prepared and characterised remains, however, sustained by only a handful of high symmetry MBBs that can be classified based by their points of extension (Figure 1). Octahedral MBBs from basic zinc acetate $[Zn_4O(CO_2)_6]$, "square paddlewheel" from $[Cu_2(CO_2)_4]$ and trigonal prismatic $[M_3(\mu_3\text{-}O)(CO_2)_6]$ clusters are predominant in this context and they sustain the majority of high-symmetry MOM networks thus far reported.

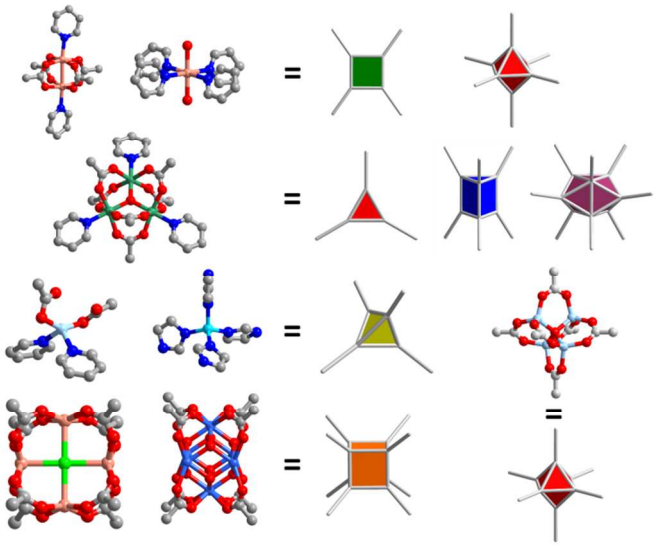

Figure 1: High symmetry Molecular Building Blocks (MBBs) that sustain prototypal MOMs and their related vertex figures.

Topology

The analysis and classification of networks in terms of topology enables delineation of the taxonomy of the underlying net[22,23] and plays an important role in crystal engineering since the observed topology is the direct consequence of linking different nodes and it provides a blueprint for design of families of related MOMs or "platforms". The process involves simplification of a crystal structure into polygons or polyhedra, nodes or vertices that are connected by linkers (or edges). The nodes of multi-atomic MBBs are represented by their centre point (barycentre). Simplification of the network and its topological analysis is readily achieved using the program TOPOS.[24] TOPOS provides point and vertex symbols of the analysed nets and identifies if a nets exhibits the same topology as one of the >70,000 known nets that are archived in its databases. In the case of MOMs, the RCSR (Reticular Chemistry Structure Resource) database[25] provides unique 3-letter codes to unambiguously describe the network topology. These network topologies can be further classified by their number of vertices: nets with one kind of vertex are called uninodal; those with two vertices binodal, and so on. The largest class of uninodal nets is afforded by one MBB and one linker (edge-transitive). They have been described as prototypal or default nets and include nets sustained by 3- (**srs**[26], **ths**[27,28]), 4- (**dia**[14,29], **nbo**[30]), 6- (**pcu**[3,28,31,32], **acs**[33]), 8- (**bcu**[34]) and 12- (**fcu**[35]) connected nodes. Binodal nets have also been exploited and, together with one kind of edge, afford versatile networks such as 3,4-c **tbo**[19,36,37] and **pto**[18,37], 4,4-c **pts**[38], 3,6-c **qom**[39] and 3,24-c **rht**.[40] All of these network topologies are well-known and robust enough to serve as blueprints for the generation of large families of related materials through judicious selection of the MBBs and linkers.

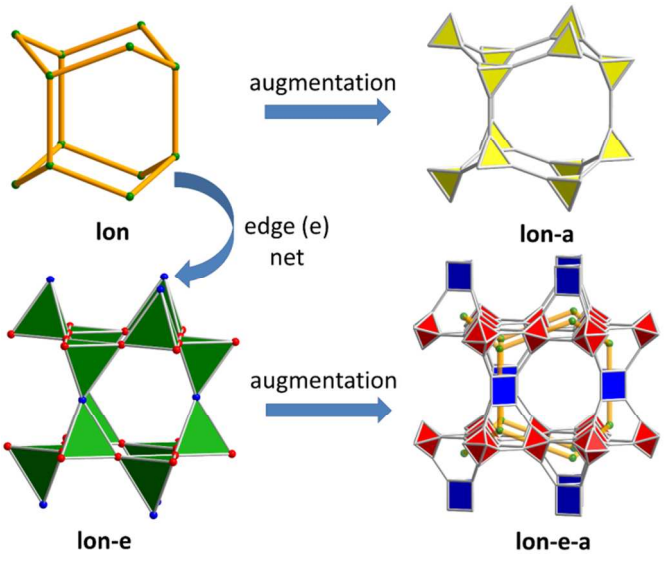

Figure 2: Relationship between the lonsdaleite (**lon**) net and its augmented (**lon-a**) and edge-nets (**lon-e**). The augmented edge-net, **lon-e-a**, is based upon both trigonal prismatic (blue) and octahedral (red) MBBs.

We would like to emphasize that description as edge or augmented nets, which detail the 'expansion' or augmentation of the parent net, respectively is important from a design perspective. Such an approach explains the topology in more detail and allows for different MBBs (or in some cases, supermolecular MBBs, SBBs) to be taken into account. For

example, lonsdaleite (**lon**)[41] topology can be used as an illustration. We recently isolated a new class of MOMs that exhibit **lon-e-a** topology.[42] In the case of **lon** topology (Figure 2, left) the tetrahedral vertex figure can be replaced by the polygon or polyhedron that defines this vertex and thus the net becomes augmented **lon** (**lon-a**). In order to generate the edge net, **lon** is expanded in a manner such that the polyhedra are directly connected whereas the linker is omitted, rendering it into a **lon-e** network. When the vertices of the **lon-e** net (green tetrahedra, Figure 2) are in turn augmented because they are sustained by different polygons or polyhedra, then the net can be described as an augmented **lon-e** net, **lon-e-a,** that is built from trigonal prismatic and octahedral nodes (Figure 2, bottom right). Similar principles apply to augmented cristobalite (**crs-a** or **dia-e-a**), which is described below and consists exclusively of octahedra.

The trigonal prismatic MBB

In this contribution we focus upon the use of the $[M_3(\mu_3\text{-}O)(O_2CR)_6]$ MBB, the "trigonal prism", which facilitates a plethora of polyhedral nets and highly porous materials, as exemplified by MIL-100[43] and MIL-101.[44] Trigonal prismatic metal-carboxylate clusters that consist of octahedral coordinated $M^{2+/3+}$ are long and well-known to coordination chemists. Basic chromium acetate was first isolated by Weinland in 1919 through treatment of hexa-aquachromium(III) chloride with sodium acetate in water or ethanol/acetic acid mixtures. The molecular formula $[Cr_3(OH)_2(O_2CCH_3)_6]Cl \cdot 8\ H_2O$ was almost correctly assigned at that time.[45] Magnetic properties were determined even before the single crystal X-ray structure was elucidated in 1965.[46]

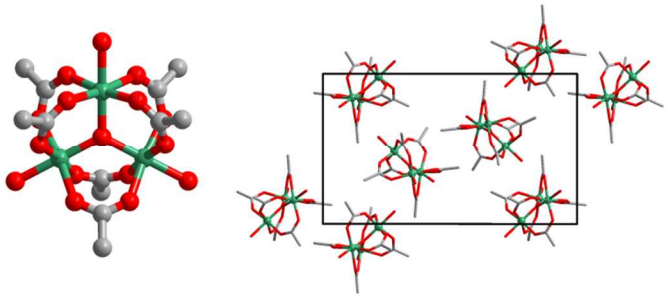

Figure 3: Single crystal structure of the basic chromium acetate trimeric cluster (left) and its packing in the orthorhombic crystal form ([001], right). Anions and water molecules are omitted due to diffuse electron density peaks.[47]

$[Cr_3(\mu_3\text{-}O)(O_2CCH_3)_6(H_2O)_3]Cl \cdot 6\ H_2O$ is composed of trimeric complex cations (Figure 3, left), that are in turn consist of three octahedrally coordinated chromium(III) ions linked to a central oxygen atom in a planar environment. In addition each Cr^{3+} is coordinated by four bridging acetate moieties and one water molecule. It crystallizes in the orthorhombic space group $P2_12_12$ with 4 formula units per unit cell. Charge balancing chloride anions and water molecules were found highly disordered between the well-refined clusters.[47] Subsequently, coordination compounds of formula $[M_3(\mu_3\text{-}O)(O_2CR)_6]X$ (X = H_2O, anion) were extensively studied because of their facile synthesis[48] and interest in their magnetic properties.

Trigonal Prisms as Building Blocks in Metal-Organic Materials

Trigonal prismatic clusters that serve as MBBs in the context of MOMs were first reported by Kim *et al.* in 2000.[49] $[Zn_3(\mu_3\text{-}O)(O_2CR)_6]N_3$ clusters connected by chiral and flexible pyridine-carboxylates afforded a 2-periodic honeycomb (**hcb**) net. Further studies on this network demonstrated enantioselective catalytic activity towards transesterification reactions. In 2002, Férey *et al.* reported the structure of the first 3-periodic network based upon $[M_3(\mu_3\text{-}O)(O_2CR)_6]$ MBBs, denoted as MIL-59.[50] The structure, which is detailed below, exhibits primitive cubic (**pcu**) topology. The first examples of linear connected trigonal prims, the MIL-88 platform,[51] were also reported by Férey and co-workers. This report was followed shortly by Yaghi *et al.*[33] who defined this hitherto unprecedented topology as the default **acs** network. A series of studies from several groups that collectively demonstrated the versatility of the trigonal prismatic MBB were subsequently reported. We herein categorize structures sustained by $[M_3(\mu_3\text{-}O)(O_2CR)_6]$ MBBs according to their connectivity. The trigonal prism can adopt one of three types of connectivity to serve as 3-, 6- or 9-connected nodes (Figure 1). The most commonly studied networks to date are 6-connected, i.e. those linked at all six carboxylate moieties, and they include structures that exhibit zeolite-like topology as well as multi-nodal networks. Multi-nodal networks are enabled by our recently reported 2-step crystal engineering strategy that exploits decorated trigonal prismatic MBBs formed in step 1 before they are further reacted with a different node(s) in step 2.

3-connected networks: 0-D Metal-organic polyhedra (MOP) and 2-D grids.

The first reports addressing the use of trigonal prismatic MBBs as 3-connected nodes for the construction of discrete metal-organic polyhedra (MOPs) were by Yaghi and co-workers. A sulfate capped MBB, $[Fe_3(\mu_3\text{-}O)(CO_2)_3(SO_4)_3]^{2-}$, was used instead of $[M_3(\mu_3\text{-}O)(CO_2)_6]^+$ and, together with linear or triangular linkers, it generated supertetrahedral SBBs, st-SBBs (IRMOPs).[52] These st-SBBs were found to be amenable to fine-tuning by means of isoreticular chemistry.[32] They were also proven to be permanently porous with BET surface areas strongly dependent upon the packing arrangement of the st-SBBs. Two main packing motifs were observed, a diamondoid (**dia**) network, as seen in MOP-54, and a less dense β-cristobalite (**crs**) net, as observed in IRMOP-51. The **crs** net served as a blueprint to connect pre-assembled st-SBBs into a 3-periodic framework. This was accomplished by connecting the unsaturated metal centres (UMCs) of the trigonal prismatic MBBs in angular fashion by 1,2-*cis*-4,4-bipyridylethane.[53] These connections render the trigonal prisms into octahedral nodes which in turn sustain the **crs-a** topology (Figure 4d). This approach greatly enhanced the stability and surface area of the material, which increased from 544 m^2/g (IRMOP-51) to 2274 m^2/g (MOF-500). This report also demonstrated the concept of a modular approach through which SBBs can be assembled into 3-D frameworks.

Another class of 3-connected MOMs is based upon linking the 3 UMCs of the trigonal prismatic MBB. The resulting networks were prepared through a 2-step synthetic approach, whereby mixed metal pivalate MBBs $[Fe_2M(\mu_3\text{-}O)(piv)_6]$ were synthesized in step 1. These MBBs were then connected through linear bipyridine[54,55] or triangular tripyridyl-linkers[56] into 2-D honeycomb (**hcb**) networks with 4-fold interpenetration. Two variants, M = Ni, Co, were found to exhibit stepwise adsorption with BET surface areas ranging from around 250 m^2/g to 550 m^2/g. Adsorption experiments with methanol and ethanol further illustrated stepwise adsorption mechanisms in these nets as, with increasing uptake,

changes in angles and distances between the interpenetrating nets were observed.

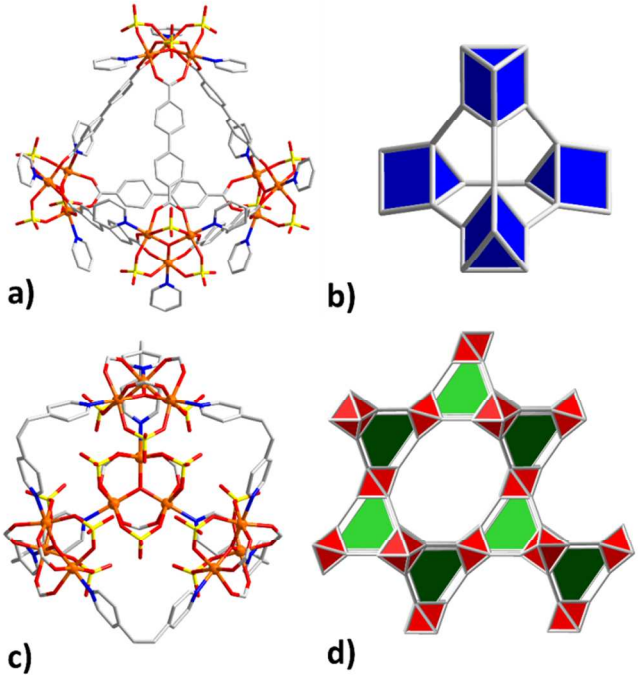

Figure 4: (a) Single crystal X-ray structure of IRMOP-51. (b) The st-SBB that is sustained by four capped trigonal prismatic MBBs; (c) connectivity between st-SBBs which renders MOF-500 into an overall (d) cristobalite (**crs-a**) net. Light and dark green tetrahedra represent the different SBBs as detailed in (a) and (c).

The **hcb** net obtained from a triangular, tripyridyl linker exhibits eclipsed ABAB packing and thus forms hexagonal channels. No flexibility was observed, resulting in a higher apparent BET surface area (730 m^2/g).[56] Flexible or angular 2-c linkers were found to afford 1-D coordination polymers or catenated chains that were shown to be non-porous.[57]

6-connected networks: MILs and others.

6-connected networks are the most common structural motifs for trigonal prismatic nodes as the structure means that their surface is decorated by six bridging carboxylate moieties. Whereas several research groups initially explored trigonal prismatic MBBs, this field has thus far been dominated by the structural diversity of MILs (Materials of Institute Lavoisier) developed by Férey, Serre and co-workers.[58] Trigonal prisms based on the highly stable Cr_3O-trimer and its Fe analogue were initially explored, resulting in highly modular platforms. Three of these platforms gained special attention thanks to their properties and potential applications: MIL-88, MIL-100 and MIL-101. MIL-88 was first reported in 2004 by linear linking of $[Fe_3(\mu_3\text{-}O)(CO_2)_6]$ MBBs by fumarate (denoted MIL-88, later MIL-88A) and *trans,trans*-muconate (denoted MIL-89).[51] Shortly thereafter, Yaghi and co-workers isolated the first network based on terephthalate linkers (bdc^{2-}) and identified the resulting topology as the 'default' net for trigonal prismatic nodes: the **acs** net.[33] The network is identical to the later reported compound MIL-88B, but differs with respect to the charge balancing anions. The MIL-88 class of frameworks (**acs** nets) were then extensively explored by Férey and co-workers by employing different linkers such as bdc^{2-} (MIL-88B), 2,6-naphthalenedicarboxylate (ndc^{2-}, MIL-88C) and 4,4-biphenyldicarboxylate ($bpdc^{2-}$, MIL-88D).[59]

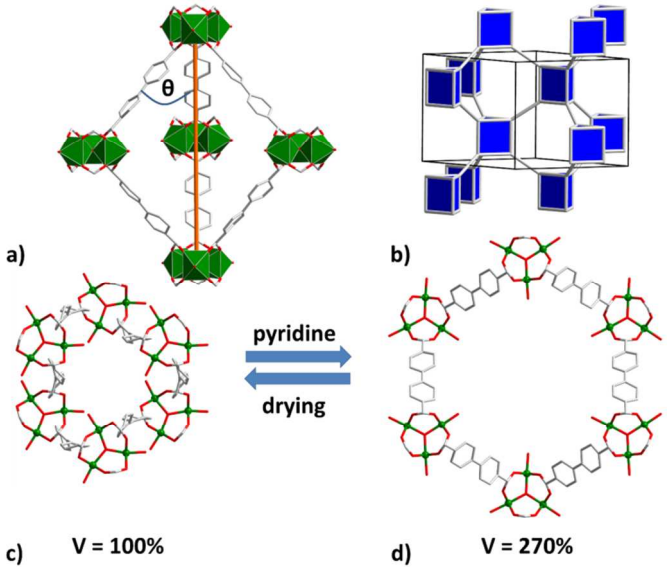

Figure 5: (a) The trigonal bipyramidal cage of MIL-88D, the angle θ changes with the swelling amplitude of the framework; (b) Default **acs** topology as exhibited by the MIL-88 family; (c) Structure of the dried form of MIL-88D and (d) after soaking in pyridine. The swelling can result in a 270% increase of unit cell volume.

These isoreticular materials were also synthesized according to a 'controlled SBU approach' starting from basic iron acetate, $[Fe_3(\mu_3\text{-}O)(O_2CCH_3)_6(H_2O)_2(OH)]$, reacted with appropriate dicarboxylate linkers at moderate temperatures. This contrasts with the synthesis of MIL-88(Cr), in which Cr-monomers are used at high temperatures under harsh synthetic conditions. The authors claim that the Fe_3O trimeric cluster remains intact during the synthesis and that only the carboxylate ligands are exchanged. Since only polycrystalline samples of MIL-88 were obtained, a combined approach of pre-modelling and Rietvelt refinement became necessary for structure elucidation. Due to the flexible nature of the trigonal prism, MIL-88 type frameworks can undergo large structural changes, breathing or swelling, upon exposure to different guest species, e.g. solvents (Figure 5c, d).[60,61] Breathing phenomena in porous materials had previously been reported.[62] However, the MIL-88 family exhibits unusually large but fully reversible swelling amplitudes with retention of crystallinity and network topology. In this context MIL-88D expands to 270% of its original unit cell volume, a value that, to the best of our knowledge, remains a record. Insights were provided to help rationalize the expansion/shrinkage on a structural level and how different solvents facilitate multi-point interactions with the framework. Further structural diversity of the MIL-88 family of frameworks was reported by other research groups using conventional or high-throughput methods. In this context, amino-functionalized[63] or anthracene-based[64] derivatives, MIL-88(Sc),[65] or MIL-88(V)[66] were also isolated.
Recently, it was shown that the swelling properties of MIL-88B and 88D could be fine-tuned by ligand modification and a series of functionalized frameworks was synthesized.[67] It was found that the size and number of functional groups strongly

affects the breathing amplitude and can ultimately lead to permanent porosity.

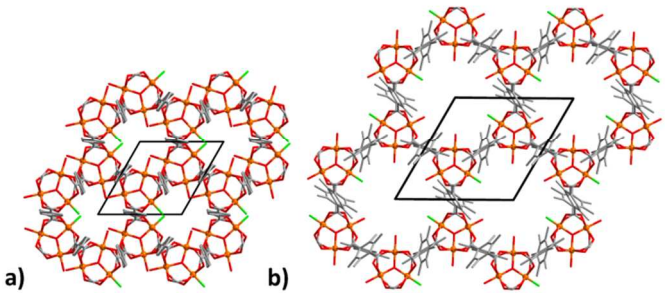

Figure 6: Simulated crystal structures of the dry forms of (a) MIL-88B and (b) MIL-88B(CH_3)$_4$. The methyl-functionalization of the 1,4-bdc linker mitigates against full shrinkage and results in increased surface area.

This was demonstrated for MIL-88B(CH_3)$_4$, the variant that contains a tetramethyl-terephthalate linker. The apparent surface area increased to 1216 m^2/g vs. < 30 m^2/g for MIL-88B (Figure 6). Moreover, it was shown that functional groups also have a profound influence on the energetics of the closed and open forms due to different host-guest interactions with solvent molecules. The lower diffusion barrier of guests in functionalized MIL-88B resulted in an unexpected breathing behaviour in non-polar solvents.

A different approach to limit or prevent breathing and yield higher surface areas in MIL-88 structures was conducted by Serre *et al.* through the synthesis of an interpenetrated version of MIL-88D, MIL-126.[68] This material, obtained through variation of the reaction conditions that produced MIL-88D, required higher temperatures and the absence of HF. It consists of 2 interwoven **acs** nets and thus its breathing amplitude upon drying is less than 2%. MIL-126 was found to be permanently porous with an apparent BET surface area of 1750 m^2/g. This study highlights how flexible, non-porous frameworks can be transformed into rigid, permanently porous structures through interpenetration.

Another important class of MILs, that deserve special attention are those with **mtn** (**M**obile **T**hirty **N**ine) topology frameworks, namely MIL-100[43] and MIL-101.[44] They are built from trigonal prismatic MBBs that, when combined with dicarboxylate or tricarboxylate ligands, form st-SBBs, similar to the aforementioned MOPs depicted in Figure 4. These st-SBBs are further linked in corner-sharing fashion[69] and thereby form 5- and 6-connected rings that result in topology the same as that of **mtn** zeolite (Figure 7). The st-SBBs are reduced to simple tetrahedral vertices in this description. However, even if the overall topology refers to the same underlying net, the particular SBB used to build a particular net must be taken into account to fully understand connectivity and make it a platform. Therefore, if MIL-101 is treated as a 6-c net it exhibits **mtn-e-a** topology whereas the 3,6-c MIL-100 net is a **moo-a** net.[23] These frameworks possess large unit cell dimensions and surface areas in the range 3100 m^2/g (MIL-100) to 5900 m^2/g (MIL-101). The properties of these extra-large surface areas were subsequently evaluated and both frameworks were found to exhibit promise with respect to storage of hydrogen,[70] carbon dioxide[71] and methane,[72] and also in drug delivery[73,74], catalysis[75,76] and gas purification.[76-78]

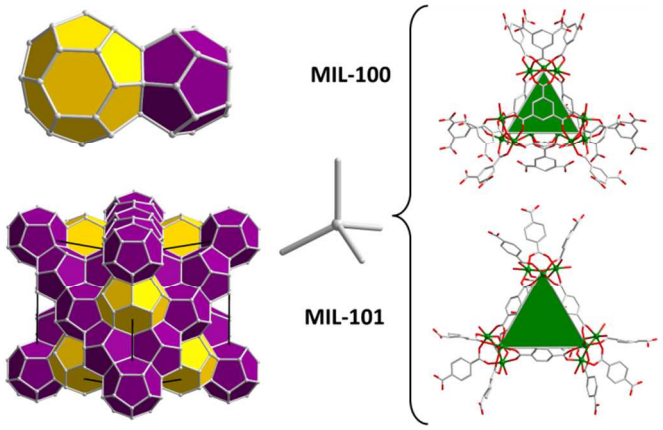

Figure 7: The underlying **mtn** topology network that sustains MIL-100 and MIL-101 consists of 2 types of cages. The nodes are different, corner-sharing supertetrahedral SBBs.

Their facile synthesis from simple building blocks, their modularity and their extra-large surface areas mean that MIL-100 and MIL-101 have attracted considerable scientific interest and variants, including MIL-101s made from Cr^{3+}[44], Fe^{3+}[78], Al^{3+}[76] and V^{3+}[66,79], have also been reported. In addition, isoreticular expansion[80] as well as ligand functionalization[81], affords many permutations of MIL-101, enabling fine-tuning for a particular application. Very recently, Stock *et al.* reported a family of single and mixed-linker functionalized Cr-MIL-101 derivatives obtained from a high-throughput approach.[81] In this context, it was found that the nature of the metal-salt, i.e. whether it is an oxide, chloride or nitrate, plays an important role in the formation of MIL-101 derivatives. The authors were also able to demonstrate that mixed linker derivatives could be used for postsynthetic modifications to further increase the diversity of functional MIL-101s.

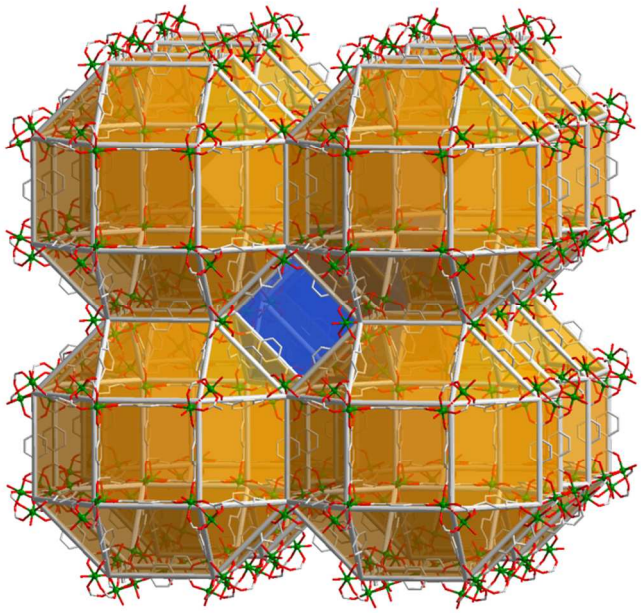

Figure 8: Predicted polymorph of MIL-101, MIL-hypo-2. The structure consists of face-sharing rhombicuboctahedral SBBs that form an **reo-e** topology net.

These postsynthetic modifications at the ligand moiety were conducted to introduce more functionality, e.g. -NO_2[82], -SO_3H[83], or more complex groups following synthesis of a functionalized framework.[74,82] Modification of UMCs, for example through amine grafting, has also enabled opportunities for metal encapsulation and catalysis.[84] In conclusion, MIL-100 and MIL-101 represent a versatile class of materials that have promise with respect to numerous applications. However, there is a minor drawback in that only microcrystalline materials are normally obtained. This means that structural information tends to be based on models and Rietveld refinement of powder x-ray data.[43,60] This limits crystal engineers although polymorphs of MIL-101 have been predicted[85] such as the **reo-e** topology net (Figure 8).[86] The **reo-e** structure is comprised of face-sharing rhombicuboctahedral SBBs which are in turn sustained by trigonal prismatic MBBs. The difference from MIL-101 lies in the different angles subtended at the particular MBBs. This framework is anticipated to show high surface area and a modular nature, but it is yet to be realised.

Besides st-SBBs, trigonal prismatic MBBs are versatile enough, because of their inherent flexibility, to form superoctahedral SBBs, so-SBBs. In this context, Zhou *et al.* reported a highly porous framework (PCN-53) based on the Fe_3O-trimer MBB and a sulphur-containing triangular ligand (H_3BTTC).[87] Two different so-SBBs generate a face-sharing arrangement to afford a novel, binodal 3,6-connected topology. The framework exhibits an apparent BET surface area of 2817 m^2/g, together with stepwise N_2-adsorption at 77K. The authors identified the primary adsorption site, supported by computational simulations, as being close to the sulphur moiety in the small octahedral cage. The other two steps were shown to have distinctive Q_{st} values. Very recently, Serre *et al.* demonstrated that a series of porous networks (MIL-142, MIL-143) can be obtained by linking different size st and so-SBBs.[88] They used a mixed ligand approach that has been shown to be fruitful for generation of high surface area materials.[89]

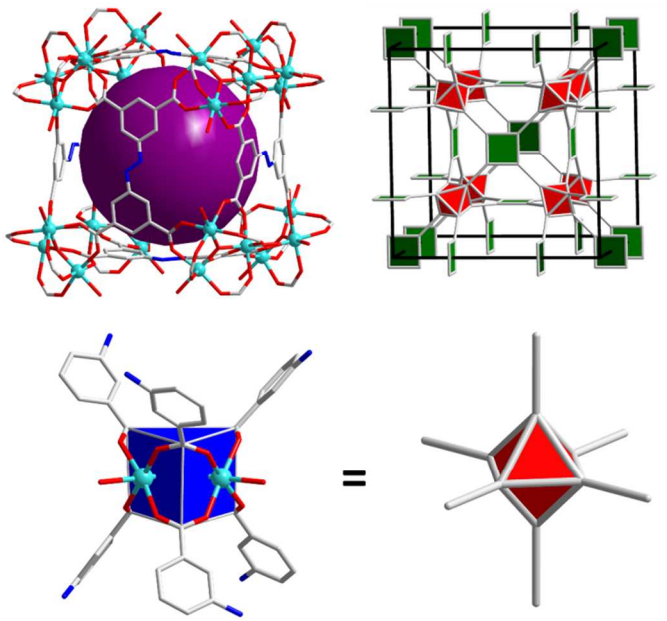

Figure 9: The single crystal x-ray structure of In-**soc**-MOF reveals a 4,6-c topology sustained by octahedra and squares (shown as **soc-a**). The octahedral vertex figure is obtained through a 120° angle at the tetracarboxylate ligand.

The resulting networks exhibit interpenetrated ReO_3 (**reo**) and β-cristobalite (**crs**) topology, respectively. MIL-142 is a platform since isoreticular expansion and the use of functionalized dicarboxylates (-NH_2, NO_2) were demonstrated. The resulting networks show apparent surface areas of around 2000 m^2/g and thus represent rare examples of materials that combine Lewis acidity, permanent porosity and organic functionalization. This study lays a foundation for mixed ligand MOMs based on trigonal prismatic nodes that could ultimately lead to materials with superior performance.

MIL-59 represents the first 3-periodic network based on the trigonal prismatic MBB [$V_3(\mu_3\text{-}O)(CO_2)_6$] that is linked with angular 1,3-bdc.[50] The structure is that of a primitive cubic **pcu** topology since the angle at the ligand (120°) compensates for the angle subtended at the trigonal prismatic MBB. In 2007, Eddaoudi *et al.* demonstrated an elegant example that uses a tetracarboxylate ligand that caps the faces of the **pcu** network, thus making it the first example of a 4,6-c **s**quare-**oc**tahedron (**soc**) topology MOM based on an Indium-trimer (Figure 9).[90] This framework exhibits a surface area of around 1400 m^2/g and high hydrogen uptake (2.61wt% at 77K). In_3O-trimers have since been widely studied in MOMs and have been found to exhibit different connectivity and topological outcomes than other trimers. Multi-nodal and zeolite-like networks are discussed separately in a later section.

9-connected networks: The ncb and xmz platforms.

High connectivity metal-organic materials are of great interest since they are likely to be more controllable than lower connectivity nets, and they can exhibit enhanced stability towards guest removal, elevated temperatures or harsh chemical conditions.

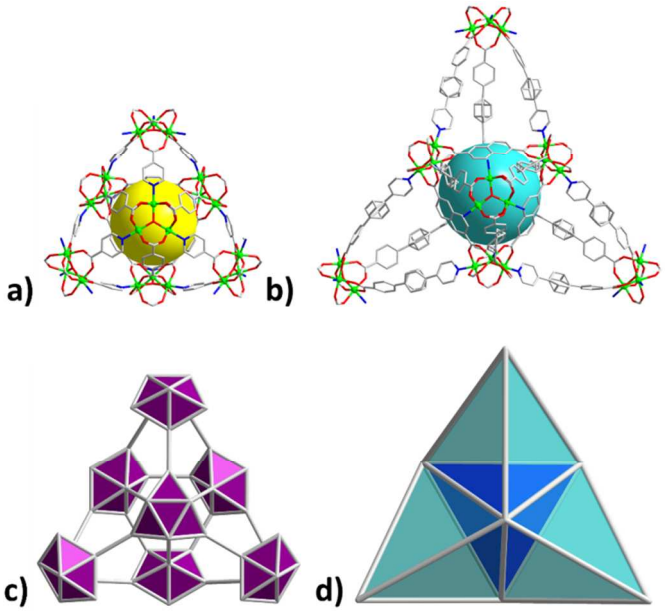

Figure 10: a) Single crystal X-ray structure of the smallest **ncb** variant based on terephthalate and iso-nicotinate; b) expanded variant of an **ncb** network; c) augmented **ncb** topology based on a 9-c vertex figure; d) tetrakis-tetrahedral cage with the tetrahedral cage in the centre of the cage.

Increasing the connectivity of a known MBB through its UMCs has been well studied in the context of square-paddlewheels (to

generate octahedra and thus **pcu** nets),[91] but it was not until 2009 that Chen *et al.* reported the first uninodal, edge-two-transitive 9-c network with the previously predicted **ncb** topology (Figure 10).[92] The use of two ligands, one dicarboxylate and one pyridine-carboxylate of right length, rendered the $[Ni_3(\mu_3\text{-}O)(CO_2)_6]py_3$ MBB into a 9-c node. The resulting network is built from a tetrakis-tetrahedron that is in turn generated from four tetrahedral cages that surround a centred tetrahedral cage (Figure 10d). The parent net, obtained through a combination of naphthalene-2,6-dicarboxylate and 4-(pyridine-4-yl)benzoate exhibits high thermal stability and a relatively high apparent BET surface area of 2316 m^2/g. In addition its hydrogen and methane uptakes were found to be relatively high. Moreover, it served as a blueprint for the generation of a large number of **ncb** networks through judicious selection of two compatible ligands.[93,94] It was further demonstrated that pore size and pore shape can be altered as well as the cavity/channel void ratio, depending on the linker combination. To assess the right linker combinations, the authors used a geometry analysis approach and thus generated a family of networks that were experimentally accessible.[93] Therefore, the **ncb** platform exhibits tuneable surface areas enabled by a crystal engineering approach that represents a fruitful strategy for the design of high connectivity platforms based on simple and readily available MBBs and linkers.

Binodal networks where the trigonal prismatic building block serves as a 9-c node were first reported in 2007 by Schröder *et al.* using a heterofunctional 3-c pyridine-dicarboxylate ligand.[95] Chen *et al.* concurrently synthesized isoreticular structures using 3,5-pyridine-dicarboxylic acid[96] (Figure 11a) and expanded variants[97] (Figure 11b). The underlying binodal, edge-two transitive topology was recently assigned the three letter code **xmz** (Figure 11d). Interestingly, **xmz** networks can be isolated with a variety of metal cations including Co[96], Fe and Ni,[95] and Mg.[98]

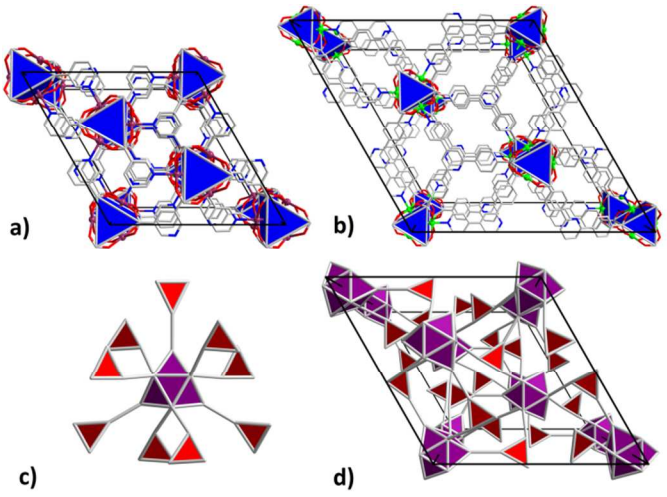

Figure 11: a) Single crystal X-ray structure of the smallest **xmz** framework; b) isoreticular expanded variant that shows framework flexibility (trigonal prismatic clusters are represented in blue); c) connectivity of the nodes (3,9-c); d) augmented **xmz** topology based on a 3-c and 9-c node with two kinds of edges (**xmz-a**).

Despite their different connectivity, **xmz** networks show similarities to the aforementioned **acs** networks in terms of symmetry and orientation of trigonal prismatic clusters within the unit cell. However, all (non-interpenetrated) **acs** nets exhibit breathing behaviour whereas this phenomenon has only been observed in one **xmz** network.[97] The authors attribute this behaviour to differences in the length of the two edges sustained by the triangular node. Specifically, no breathing is observed when the edge lengths are very different (Figure 11a) whereas edges of similar length (Figure 11b) facilitate breathing upon solvent exchange or removal as well as upon temperature change. The observed breathing amplitudes ranged from 70 to 105% of the unit cell volume.

Multi-nodal networks: Zeolite-like materials.

In this section, we mainly focus on multi-nodal networks that cannot be clearly categorized in terms of connectivity and deserve special attention since their underlying structure is zeolitic. MBBs constructed from In^{3+} have afforded a structurally diverse range of MOMs with anionic tetrahedral $[In(CO_2)_4]^{-}$[99] MBBs and cationic trigonal prismatic $[In_3(\mu_3\text{-}O)(CO_2)_6]^{+}$[100] MBBs representing the primary examples. In 2010, Bu *et al.* reported elegant examples of zeolite-like structures (CPM-5)[101] sustained by such polyhedra linked by triangular btc^{3-} nodes. Trigonal prismatic MBBs form st-SBBs (Figure 12, left) that are nested within a sodalite, **sod**, cage sustained by tetrahedral nodes (Figure 12, right).

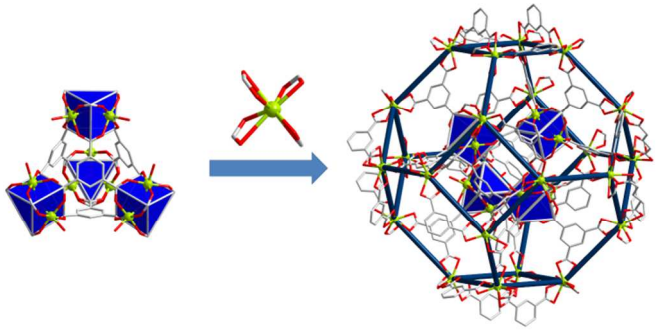

Figure 12: The st-SBB formed by In_3O-trimers linked by btc^{3-} in CPM-5 (left). Peripheral carboxylates coordinate to tetrahedral $In(CO_2)_4^{-}$ nodes that form a **sod** cage (right).

This results in a pore partitioning effect which, together with the presence of UMCs and the anionic charge of the framework, facilitates high uptake of carbon dioxide and, especially, hydrogen, even though the apparent BET surface area is relatively low (580 m^2/g). A related structure with **sod** topology and two distinct **sod** cages was reported in 2012.[102] One cage is very similar to those which sustain CPM-5 and contains In/M_3O (M = Mg, Mn, Co, Ni, Cd) mixed metal trimers. The other cage contains M_3O trimers that serve only as 3-connected nodes and are dangling into the sodalite cage. The apparent surface area and uptakes for carbon dioxide and hydrogen were lower than CPM-5, however a high CO_2/N_2 selectivity was observed. In addition to the examples detailed above, In_3O-trimers are versatile enough to sustain diverse nets[103] with branched or functionalized ligands, including **nia**,[104] or **acs** nets with entrapped metal clusters.[105]

2-step Crystal Engineering: New families of multi-nodal frameworks.

As previously mentioned, MOMs constructed from trigonal prismatic MBBs are chemically robust and structurally rigid. However, especially in the case of chromium, they tend to form

microcrystalline powders. This is exemplified by the dearth of 3-periodic networks containing the $[Cr_3(\mu_3\text{-}O)(CO_2)_6]$ trigonal prism that have been investigated by single crystal X-ray diffraction. Rather, structure solutions derived from powder diffraction data have tended to be utilized, thereby inhibiting the study of subtle structural features. Recently, we addressed this matter through a 2-step crystal engineering strategy[106] that relies on preformation of a decorated MBB which is subsequently connected through a different metal node to yield 3-D network structures. 2-step synthetic strategies were previously known in the context of MOMs[107] and have great potential to increase structural diversity. However, they remain largely unexplored. Our 2-step synthetic approach involves isolation of a trigonal prismatic primary molecular building block (tp-PMBB-1) in the first step. In the second step, this highly soluble tp-PMBB is dissolved and coordinated to various metal cations through its six exodentate pyridyl moieties (Figure 13). We initially explored nets that are cationic since they are sustained by both metal-carboxylate and metal-pyridine bonds. The first three isolated examples were found to exhibit **snx**, **snw** and **stp** topologies respectively, with the second metal cation being Ag^+ or Cd^{2+}.

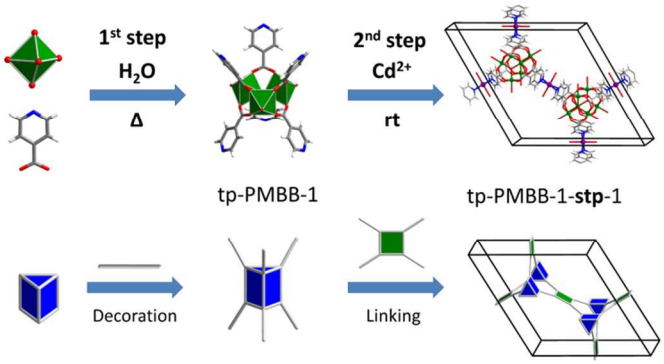

Figure 13: Schematic of the 2-step crystal engineering strategy that afforded tp-PMBB-1-**stp**-1. The tp-PMBB is prepared (decorated) in step 1 and then linked to Cd^{2+} at room temperature in step 2.

Since **stp** networks possess a modular nature and contain exchangeable anions in the nanoporous channels, we selected this particular topology as a blueprint for the generation of a new MOM platform.[108] Three other decorated tp-PMBBs were synthesized and we were able to demonstrate the generality of the 2-step strategy in an isoreticular fashion. In this context, the tp-PMBBs formed by nicotinate[109] (tp-PMBB-2), -(4-pyridyl)benzoic acid (tp-PMBB-3) and *trans*-3-(3-pyridyl)acrylic acid (tp-PMBB-4) were isolated. After rendering these MBBs into **stp** topology MOMs, the pore size was increased up to 3.0 nm (tp-PMBB-3-**stp**-1), which has thus far been seen in only a few MOMs.[110] In addition, selective binding of large organic anionic guests was observed to induce a breathing effect in tp-PMBB-4-**stp**-1 during single crystal-to-single crystal (SCSC) transformations. In contrast, small inorganic anions or the use of various solvents did not change the cell parameters. We also demonstrated that anion exchange in a cationic **acs** net, tp-PMBB-2-**acs**-1, can profoundly impact gas sorption performance towards carbon dioxide with a >250% increase in uptake. The 2-step crystal engineering strategy was also recently employed to generate two novel frameworks with **acs** and **stp** topologies that are based on two types of MBB,[111] an amino-benzoate decorated Cr_3O-trimer MBB and a $[Cu_3(\mu_3\text{-}Cl)(NH_2\text{-}R)Cl_6]$-cluster that had hitherto not been used in MOMs. Different connectivity of the decorated tp-PMBBs resulted in free amino-groups lining the hexagonal channels of the **stp** net that exhibits enhanced affinity for CO_2.

In contrast to uninodal and binodal networks, trinodal networks composed of three different polygons or polyhedra are scarce and no versatile platform has yet emerged. This might be associated with the difficulty of controlling a self-assembly process when several competing functional groups are present in a one-pot reaction.

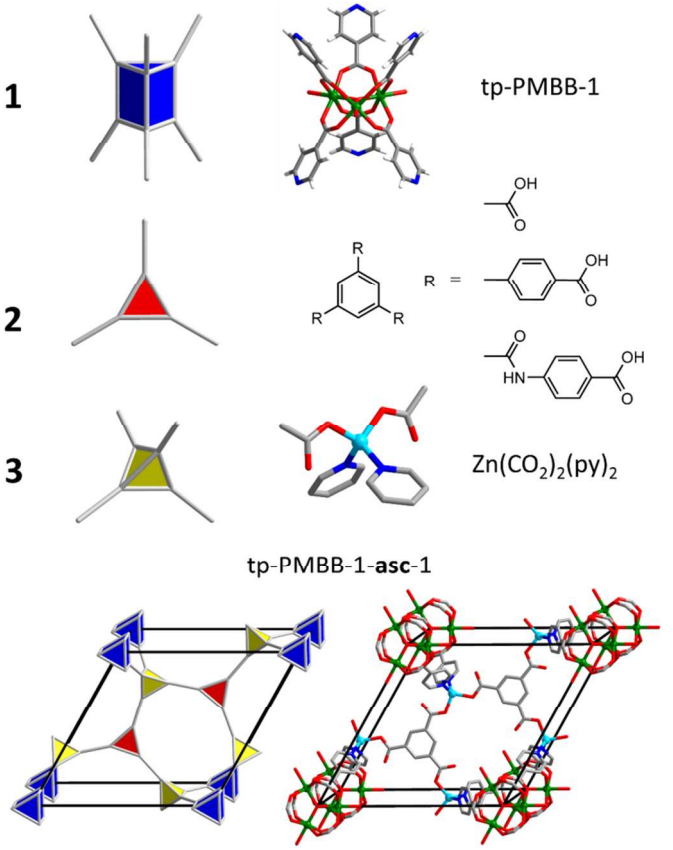

Figure 14: Self-assembly of a trinodal net. A preformed trigonal prismatic MBB (tp-PMBB-1) is reacted in step 2 with Zn^{2+} tetrahedral and btc^{3-} triangles to afford the trinodal 3,4,6-c **asc** network.

We applied our 2-step strategy to three nodes by linking tp-PMBB-1 to tetrahedral Zn^{2+} cations which in turn coordinate to two triangular btc^{3-} anions (Figure 14). The resulting network represents the first MOM with the trinodal 3,4,6-connected **asc** topology, tp-PMBB-1-**asc**-1.[112] These networks are platforms since network components could be systematically varied with retention of topology. Specifically, tetrahedral Zn^{2+} was substituted by tetrahedral Cd^{2+} cations and triangular btc^{3-} anions were replaced by expanded variants such as 1,3,5-tris(4-carboxyphenyl) benzene (btb^{3-}) or 4,4',4''-[1,3,5-benzenetriyltris(carbonylimino)] trisbenzoic acid ($btctb^{3-}$). The resulting structures contained nanocages of dimensions 39 x 19 Å (btb^{3-}) and 47 x 23 Å ($btctb^{3-}$). The parent structure, tp-PMBB-1-**asc**-1, is permanently porous (BET: 1671 m^2/g) and shows moderately strong uptake for carbon dioxide (273, 298K) and hydrogen (77K). More importantly, from a practical perspective, tp-PMBB-1-**asc**-1 exhibits chemical stability in hot

organic bases and water, a challenging but relevant requirement with respect to most industrial applications of porous materials.[113] Solvent molecules also represent an opportunity for fine-tuning the pore walls and sorption properties since, when crystals of tp-PMBB-1-**asc**-1 were immersed in hot pyridine, it was found that the terminal water ligands could be exchanged for pyridine ligands in a SCSC transformation. Soaking of crystals in water for several days and subsequent activation indicated no loss of surface area. The **asc** network is therefore highly versatile since it offers several approaches to fine-tuning of structure and properties. This enables systematic structure/function studies that are important both fundamentally and practically.

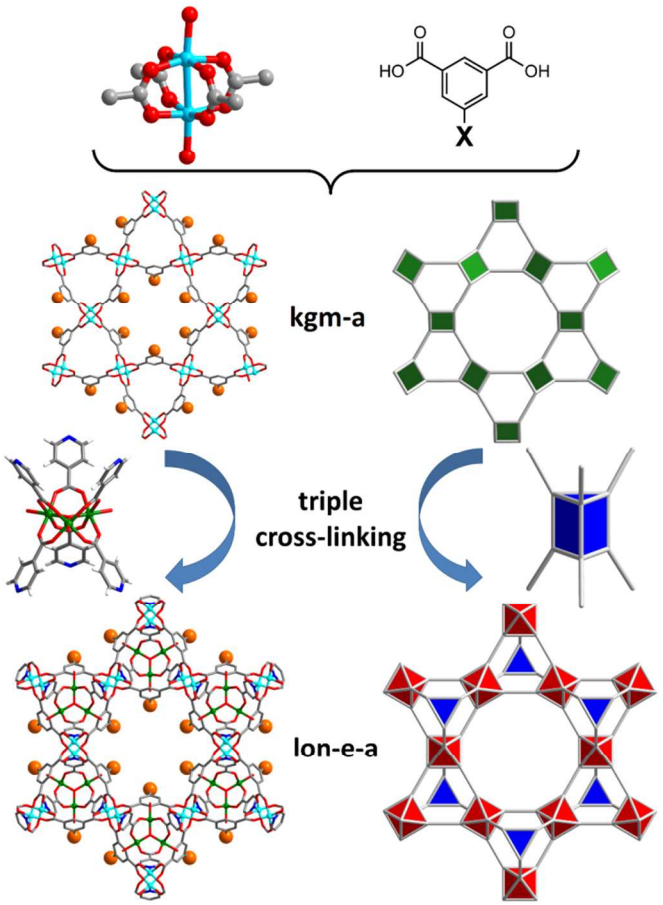

Figure 15: Self-assembly of functionalized **lon-e-a** networks. A 2-periodic undulating **kgm** lattice is triply cross-linked by tp-PMBB-1 to afford an eclipsed arrangement of layers and hexagonal pores along [001]. Orange spheres represent the 5-position of 1,3-bdc linkers, a site that is readily fine-tuned.

Very recently, we utilized our 2-step approach to address a new pillaring strategy for undulating kagomé (**kgm**) networks[114] which transforms them into a new and versatile class of 3-periodic MOMs with augmented lonsdaleite-e (**lon-e-a**) topology (Figure 15).[115] The **kgm** network was generated using all of 9 different angular linkers, including 1,3-bdc with various functional groups at its 5-position and 2,5-furandicarboxylate. From a crystal engineering perspective, we took advantage of the flexible nature of tp-PMBB-1 to facilitate a fit with the three tilted paddlewheel moieties of the 2-D **kgm** net. The resulting st-SBBs are connected in a corner-sharing fashion and thus afford a **lon-e-a** network with hexagonal channels along [001]. These channels are lined by the functional groups that lie at the 5-position of the 1,3-bdc ligands.

Table 1: A tabulation of the compounds discussed in this perspective presenting the following parameters: underlying topology; angle subtended at the trigonal prismatic MBB; REFCODE retrieved from CSD.[116] ([a]C-μ_3O-S angle, [b]ligand geometry highly disordered, [c]overall topology considering only tetrahedral nodes, [d]cif-file was retrieved from the supporting information, [e]**lon-e** variants exhibit C-μ_3O-C angles within 1°).

compound	topol.	C-μ_3O-C angle			REFCODE	ref.
Cr-acetate	-	68.4	71.7	72.8	CRACOP11	47
D-POST-1	**hcb**	76.1			UHOPUC	49
MIL-59	**pcu**	75.0			XOFFUT	50
MIL-59(In)	**pcu**	74.1			RIDCAJ	90
acs (1,4-bdc)	**acs**	77.8			DANWOF	33
acs (1,3-bdc)	**acs**	68.8			DANWUL	33
IRMOP-51[a]	**crs**	65.7			JANZEE01	52
MOF-500[a]	**crs**	66.3			ICITEU	53
FeNi-piv-bipy	**hcb**	76.1	68.0	67.8	ILUXIX	55
MIL-88B	**acs**	80.7			YEDKOI	59
MIL-88C[b]	**acs**	96.1			YEDLAV	59
MIL-88D (close)	**acs**	78.0			YEDKUO	59
MIL-88D (open)	**acs**	86.1			REZXUQ	61
MIL-88B_NH_2	**acs**	79.1			KOKKOL	63
MIL-88B$(CH_3)_4$	**acs**	72.6			SI[d]	67
PCN-19	**acs**	71.7			KUGZIW	64
MIL-100	**moo**	84.0	80.4	74.8	UDEMEW	43
		74.6	72.6	67.7		
		63.5				
MIL-101	**mtn-e**	81.9	75.9	74.3	OCUNAC	44
		69.2	68.7	68.2		
		63.4	61.4			
MIL-hypo-2	**reo-e**	70.2	68.1		IZEPAF	86
In-**soc**-MOF	**soc**	69.5			RIDCEN	90
ncb - Ia	**ncb**	68.1			KARLAS	93
ncb - IIa	**ncb**	71.6			KARLEW	93
ncb - IIb	**ncb**	69.6			KARLIA	93
ncb - IIIa	**ncb**	73.9			KARLOG	93
ncb - IIIb	**ncb**	70.6			KARLUM	93
ncb - IIIc	**ncb**	67.9			KARMAT	93
ncb - IVa	**ncb**	73.3			KARMEX	93
ncb - IVb	**ncb**	71.1			KARMIB	93
ncb - IVc	**ncb**	69.0			KARMOH	93
ncb - Va	**ncb**	78.3			KARMUN	93
ncb - Vb	**ncb**	72.8			KARNAU	93
ncb - Vc	**ncb**	70.8			KARNEY	93
ncb - Vd	**ncb**	68.8			KARNIC	93
Co-**xmz** (small)	**xmz**	57.5			EDAJUP	96
Ni-**xmz** (med.)	**xmz**	74.6			VEXTUO	95
Ni-**xmz** (large)	**xmz**	60.7			SI[d]	97
CPM-5	**sod**[c]	70.9			IMUTUG	101
CPM-15-Mg	**sod**[c]	69.0			HANKAK	102
tp-PMBB-1-**snx**-1	**snx**	70.9	67.7		BIGZUO	106
snw-1	**snw**	75.1	69.3	67.7	BIHBAX	106
stp-1	**stp**	72.0			SI[d]	106
asc-1	**asc**	73.9			SETSIV	112
asc-1-py	**asc**	74.6			SETSOB	112
asc-2	**asc**	71.1			SETSUH	112
asc-3	**asc**	69.8			SETTAO	112
lon-e[e]	**lon-e**	76.7			SI[d]	42

This platform was systematically studied in terms of gas sorption performance with respect to carbon dioxide. The surface areas of the variants are considerably different but the uptakes were observed to correlate with functionality rather than surface area with the following trend: *t*-Bu > H ≈ fdc ≈ NO_2 > Br. This trend agrees with studies conducted upon functionalized DMOFs.[117] We also investigated the effect of functional groups on methane adsorption and found a considerable increase in affinity when pore walls are lined with alkyl-groups and pore space is smaller. The observed heats of adsorption, Q_{st}, of the best performing variants were found to be amongst the highest values reported to date[118] and validate the use of alkyl groups to enhance methane-framework interactions.

In summary the 2-step synthetic strategy can generate charged networks from trigonal prismatic MBBs that possess large solvent accessible channels that enable facile anion exchange. Further, this inherently modular approach enables precise control over the assembly process that cannot be so easily achieved in one-pot reactions, thereby facilitating generation of new multi-nodal platforms. These multi-nodal platforms offer systematic structure/property studies.

The importance of breathing effects in nets based upon nets based upon trigonal prismatic MBBs.

The structural diversity of trigonal prismatic nets can be mainly attributed to the flexible nature of the MBB as it can accommodate a wide variety of C-μ_3O-C angles ranging from 86.6° (MIL-88D, open form) to 57.7° (Co-**xmz**). The angles reported herein were retrieved from the Cambridge Structural Database (CSD)[116] and are summarized in Table 1. Flexible MBBs are rarely encountered in the realm of metal-carboxylate clusters and there are parallels to zeolite chemistry, for which the variability of M-O-M angles enables the diverse range of secondary building units and complex building units needed to build a range of zeolitic nets.[5] M-O-M angles (typically in a range of 140° to 165°) in zeolitic primary building units (PBUs) lead to a variety of ring sizes that can serve as secondary building units (SBUs). In a similar manner, that a range of angles can be subtended at trigonal prismatic MBBs facilitates the existence of families of SBBs. This in turn enables framework diversity of the type detailed herein. We consider that this feature makes trigonal prismatic MBBs particularly attractive to crystal engineers as they target new platforms. In addition, the flexible nature of the MBB enables shrinking and expansion of the framework over large magnitudes as exemplified by the MIL-88 family (Table 1). Such flexibility, when coupled with structural and compositional diversity, will afford porous materials with fine-tuneable structural features and bulk properties, making them especially relevant with respect to gas sorption performance and sensing applications.

Conclusions

Metal-organic materials, MOMs, also known as porous coordination polymers (PCPs) or metal-organic frameworks (MOFs), are open networks generally comprised of metal cations, metal cluster or molecular MBBs connected by organic or inorganic linkers. They represent a class of porous materials that have captured the imagination of researchers worldwide because they can be designed from first principles and they exhibit unprecedented surface area. Whereas initial contributions in the field tended to focus on metal-pyridine coordination environments, metal-carboxylate cluster MBBs soon dominated thanks to their greater structural diversity in terms of accessible polygons and polyhedra. They also offer greater scale, ready accessibility and relative stability, resulting in extra-large surface area and permanent porosity. However, although there are now thousands, if not tens of thousands, of MOMs known, only a small number of them represent platforms that are amenable to fine-tuning that in turn enables the systematic study of structure and function. In this context, MBBs based upon the $[M_3(\mu_3\text{-}O)(O_2CR)_6]$ trigonal prism are notable not just for their historical contributions but for their strong potential for contributing to the future of MOMs. This is because of several reasons:

- They are particularly facile to prepare from inexpensive building blocks.
- The resulting networks tend to exhibit excellent chemical stability and strong performance with respect to gas sorption behaviour.
- MOMs sustained by high connectivity MBBs tend to provide greater control over structure as well as higher thermal and chemical stability. This trend is evident in the recent literature, which has seen an increased number of even higher connectivity MOMs.
- They contain UMCs that can be used for pore size control, pore chemistry control or for higher connectivity.[85,86]
- They offer one additional feature that makes them even more versatile than most other clusters, their flexibility that is reminiscent of a "butterfly effect". This effect can cause collapse in uninodal nets but it can also facilitate the formation of supertetrahedral and superoctahedral SBBs that would otherwise be geometrically strained and it enables new classes of multi-nodal nets that offer extraordinary diversity in terms of fine-tuning.

Therefore, although trigonal prismatic structures remain less exploited than other polynuclear clusters in coordination chemistry, in general, and porous materials science, in particular, the facile synthesis and structural versatility of $[M_3(\mu_3\text{-}O)(O_2CR)_6]$ clusters means that this long-known family of compounds has been playing an increasingly visible role in MOM design. There is every expectation that this trend will continue, especially as the challenges to further development of MOMs become more related to practical matters such as cost and stability.

Notes and references

[a] Department of Chemistry, University of South Florida, 4202 East Fowler Ave., CHE205, Tampa, Florida 33620, United States.
[b] Department of Chemical and Environmental Science, University of Limerick, Limerick, Ireland.

1 B. Moulton, M. J. Zaworotko, *Chemical Reviews*, 2001, **101**, 1629-1658; S. Kitagawa, R. Kitaura, S.-i. Noro, *Angewandte Chemie International Edition*, 2004, **43**, 2334-2375; C. Janiak, *Dalton Transactions*, 2003, 2781-2804;A. J. Blake, N. R. Champness, P. Hubberstey, W.-S. Li, M. A. Withersby, M. Schröder, *Coordination Chemistry Reviews*, 1999, **183**, 117-138; S. L. James, *Chemical Society Reviews*, 2003, **32**, 276-288.

2 S. R. Batten, R. Robson, *Angewandte Chemie International Edition*, 1998, **37**, 1460-1494.

3 M. Eddaoudi, D. B. Moler, H. Li, B. Chen, T. M. Reineke, M. O'Keeffe, O. M. Yaghi, *Accounts of Chemical Research*, 2001, **34**, 319-330.

4 H. Furukawa, K. E. Cordova, M. O'Keeffe, O. M. Yaghi, *Science*, 2013, **341**.
5 C. Baerlocher, L. B. McCusker, D. H. Olson, *Atalas of Zeolite Framework Types*, 6th revised ed.; Elsevier Science: Amsterdam, 2007.
6 L. J. Murray, M. Dincă, J. R. Long, *Chemical Society Reviews*, 2009, **38**, 1294; K. Sumida, D. L. Rogow, J. A. Mason, T. M. McDonald, E. D. Bloch, Z. R. Herm, T.-H. Bae, J. R. Long, *Chemical Reviews*, 2012, **112**, 724-781.
7 J. Lee, O. K. Farha, J. Roberts, K. A. Scheidt, S. T. Nguyen, J. T. Hupp, *Chemical Society Reviews*, 2009, **38**, 1450; L. Ma, C. Abney, W. Lin, *Chemical Society Reviews*, 2009, **38**, 1248.
8 B. Chen, S. Xiang, G. Qian, *Accounts of Chemical Research*, 2010, **43**, 1115-1124; J.-R. Li, J. Sculley, H.-C. Zhou, *Chemical Reviews*, 2011, **112**, 869-932.
9 L. E. Kreno, K. Leong, O. K. Farha, M. Allendorf, R. P. Van Duyne, J. T. Hupp, *Chemical Reviews*, 2011, **112**, 1105-1125; Y. Cui, Y. Yue, G. Qian, B. Chen, *Chemical Reviews*, 2011, **112**, 1126-1162.
10 G. R. Desiraju, *Crystal Engineering. The Design of Organic Solids*, Elsevier, Amsterdam, 1989.
11 A. Wells, *Acta Crystallographica*, 1954, **7**, 535-544; A. Wells, *Acta Crystallographica*, 1954, **7**, 545-554; B. F. Hoskins, R. Robson, *Journal of the American Chemical Society*, 1989, **111**, 5962-5964.
12 G. B. Gardner, D. Venkataraman, J. S. Moore, S. Lee, *Nature*, 1995, **374**, 792-795.
13 B. F. Hoskins, R. Robson, *Journal of the American Chemical Society*, 1990, **112**, 1546-1554; O. Ermer, *Advanced Materials*, 1991, **3**, 608-611.
14 M. J. Zaworotko, *Chemical Society Reviews*, 1994, **23**, 283-288.
15 M. Fujita, Y. J. Kwon, S. Washizu, K. Ogura, *Journal of the American Chemical Society*, 1994, **116**, 1151-1152.
16 S. Subramanian, M. J. Zaworotko, *Angewandte Chemie International Edition in English*, 1995, **34**, 2127-2129.
17 L. Carlucci, G. Ciani, D. M. Proserpio, *Coordination Chemistry Reviews*, 2003, **246**, 247-289.
18 B. Chen, M. Eddaoudi, S. T. Hyde, M. O'Keeffe, O. M. Yaghi, *Science*, 2001, **291**, 1021-1023.
19 S. S. Y. Chui, S. M. F. Lo, J. P. H. Charmant, A. G. Orpen, I. D. Williams, *Science*, 1999, **283**, 1148-1150.
20 H. Li, M. Eddaoudi, T. L. Groy, O. M. Yaghi, *Journal of the American Chemical Society*, 1998, **120**, 8571-8572.
21 M. Kondo, T. Yoshitomi, H. Matsuzaka, S. Kitagawa, K. Seki, *Angewandte Chemie International Edition in English*, 1997, **36**, 1725-1727.
22 N. W. Ockwig, O. Delgado-Friedrichs, M. O'Keeffe, O. M. Yaghi, *Accounts of Chemical Research*, 2005, **38**, 176-182; E. V. Alexandrov, V. A. Blatov, A. V. Kochetkov, D. M. Proserpio, *CrystEngComm*, 2011, **13**, 3947-3958; M. Li, D. Li, M. O'Keeffe, O. M. Yaghi, *Chemical Reviews*, 2013, **114**, 1343-1370.
23 M. O'Keeffe, O. M. Yaghi, *Chemical Reviews*, 2012, **112**, 675-702.
24 V. A. Blatov, , *IUCrCompComm Newsletter* 2006, **7**, 4-38; http://www.topos.samsu.ru
25 M. O'Keeffe, M. A. Peskov, S. J. Ramsden, O. M. Yaghi, *Accounts of Chemical Research*, 2008, **41**, 1782-1789; http://rcsr.anu.edu.au/.
26 L. Carlucci, G. Ciani, D. M. Proserpio, A. Sironi, *Journal of the American Chemical Society*, 1995, **117**, 12861-12862; N. L. Rosi, J. Kim, M. Eddaoudi, B. Chen, M. O'Keeffe, O. M. Yaghi, *Journal of the American Chemical Society*, 2005, **127**, 1504-1518.
27 L. Carlucci, G. Ciani, D. M. Proserpio, A. Sironi, *Journal of the American Chemical Society*, 1995, **117**, 4562-4569.
28 C. Bonneau, O. Delgado-Friedrichs, M. O'Keeffe, O. M. Yaghi, *Acta Crystallographica Section A*, 2004, **60**, 517-520.
29 O. R. Evans, W. B. Lin, *Accounts of Chemical Research*, 2002, **35**, 511-522.
30 M. Eddaoudi, J. Kim, M. O'Keeffe, O. M. Yaghi, *Journal of the American Chemical Society*, 2002, **124**, 376-377; B. Chen, N. W. Ockwig, A. R. Millward, D. S. Contreras, O. M. Yaghi, *Angewandte Chemie International Edition*, 2005, **44**, 4745-4749.
31 H. Li, M. Eddaoudi, M. O'Keeffe, O. M. Yaghi, *Nature*, 1999, **402**, 276-279.
32 M. Eddaoudi, J. Kim, N. Rosi, D. Vodak, J. Wachter, M. O'Keeffe, O. M. Yaghi, *Science*, 2002, **295**, 469-472.
33 A. C. Sudik, A. P. Côté, O. M. Yaghi, *Inorganic Chemistry*, 2005, **44**, 2998-3000.
34 D.-L. Long, A. J. Blake, N. R. Champness, C. Wilson, M. Schröder, *Angewandte Chemie International Edition*, 2001, **40**, 2443-2447; O. Delgado Friedrichs, M. O'Keeffe, O. M. Yaghi, *Acta Crystallographica Section A*, 2003, **59**, 22-27; Q.-R. Fang, G.-S. Zhu, Z. Jin, M. Xue, X. Wei, D.-J. Wang, S.-L. Qiu, *Angewandte Chemie International Edition*, 2006, **45**, 6126-6130.
35 J. H. Cavka, S. Jakobsen, U. Olsbye, N. Guillou, C. Lamberti, S. Bordiga, K. P. Lillerud, *Journal of the American Chemical Society*, 2008, **130**, 13850-13851; H.-N. Wang, X. Meng, G.-S. Yang, X.-L. Wang, K.-Z. Shao, Z.-M. Su, C.-G. Wang, *Chemical Communications*, 2011, **47**, 7128-7130.
36 S. Ma, D. Sun, M. Ambrogio, J. A. Fillinger, S. Parkin, H.-C. Zhou, *Journal of the American Chemical Society*, 2007, **129**, 1858-1859.
37 H. Furukawa, Y. B. Go, N. Ko, Y. K. Park, F. J. Uribe-Romo, J. Kim, M. O'Keeffe, O. M. Yaghi, *Inorganic Chemistry*, 2011, **50**, 9147-9152.
38 B. Chen, M. Eddaoudi, T. M. Reineke, J. W. Kampf, M. O'Keeffe, O. M. Yaghi, *Journal of the American Chemical Society*, 2000, **122**, 11559-11560; J. Kim, B. Chen, T. M. Reineke, H. Li, M. Eddaoudi, D. B. Moler, M. O'Keeffe, O. M. Yaghi, *Journal of the American Chemical Society*, 2001, **123**, 8239-8247.
39 H. K. Chae, D. Y. Siberio-Perez, J. Kim, Y. Go, M. Eddaoudi, A. J. Matzger, M. O'Keeffe, O. M. Yaghi, *Nature*, 2004, **427**, 523-527.
40 F. Nouar, J. F. Eubank, T. Bousquet, L. Wojtas, M. J. Zaworotko, M. Eddaoudi, *Journal of the American Chemical Society*, 2008, **130**, 1833-1835; B. Zheng, J. Bai, J. Duan, L. Wojtas, M. J. Zaworotko, *Journal of the American Chemical Society*, 2010, **133**, 748-751; O. K. Farha, I. Eryazici, N. C. Jeong, B. G. Hauser, C. E. Wilmer, A. A. Sarjeant, R. Q. Snurr, S. T. Nguyen, A. Ö. Yazaydın, J. T. Hupp, *Journal of the American Chemical Society*, 2012, **134**, 15016-15021.
41 O. M. Yaghi, M. O'Keeffe, N. W. Ockwig, H. K. Chae, M. Eddaoudi, J. Kim, *Nature*, 2003, **423**, 705; D. M. Ciurtin, M. D. Smith, H.-C. z. Loye, *Chemical Communications*, 2002, 74-75; B. Sreenivasulu, J. J. Vittal, *Crystal Growth & Design*, 2003, **3**, 635-637.
42 A. Schoedel, W. Boyette, L. Wojtas, M. Eddaoudi, M. J. Zaworotko, *Journal of the American Chemical Society*, 2013, **135**, 14016-14019.
43 G. Férey, C. Serre, C. Mellot-Draznieks, F. Millange, S. Surblé, J. Dutour, I. Margiolaki, *Angewandte Chemie International Edition*, 2004, **43**, 6296-6301.

44 G. Férey, C. Mellot-Draznieks, C. Serre, F. Millange, J. Dutour, S. Surblé, I. Margiolaki, *Science*, 2005, **309**, 2040-2042.
45 R. F. Weinland, *Einfuehrung in die Chemie der Komplex Verbindungen*, Stuttgart, 1919.
46 B. N. Figgis, G. B. Robertson, *Nature*, 1965, **205**, 694-695.
47 S. C. Chang, G. A. Jeffrey, *Acta Crystallographica Section B*, 1970, **26**, 673-683.
48 B. J. Hathaway, *Comprehensive Coordination Chemistry*, Vol. 2 (Ed. G. Wilkinson), Pergamon, Oxford, 1987.
49 S. Jung Soo, W. Dongmok, L. Hyoyoung, J. Sung Im, O. Jinho, J. Young Jin, K. Kimoon, *Nature*, 2000, **404**, 982.
50 K. Barthelet, D. Riou, G. Férey, *Chemical Communications*, 2002, 1492-1493.
51 C. Serre, F. Millange, S. Surblé, G. Férey, *Angewandte Chemie International Edition*, 2004, **43**, 6285-6289.
52 A. C. Sudik, A. R. Millward, N. W. Ockwig, A. P. Côté, J. Kim, O. M. Yaghi, *Journal of the American Chemical Society*, 2005, **127**, 7110-7118.
53 A. C. Sudik, A. P. Côté, A. G. Wong-Foy, M. O'Keeffe, O. M. Yaghi, *Angewandte Chemie International Edition*, 2006, **45**, 2528-2533.
54 R. A. Polunin, S. V. Kolotilov, M. A. Kiskin, O. Cador, E. A. Mikhalyova, A. S. Lytvynenko, S. Golhen, L. Ouahab, V. I. Ovcharenko, I. L. Eremenko, V. M. Novotortsev, V. V. Pavlishchuk, *European Journal of Inorganic Chemistry*, 2010, 5055-5057.
55 R. A. Polunin, S. V. Kolotilov, M. A. Kiskin, O. Cador, S. Golhen, O. V. Shvets, L. Ouahab, Z. V. Dobrokhotova, V. I. Ovcharenko, I. L. Eremenko, V. M. Novotortsev, V. V. Pavlishchuk, *European Journal of Inorganic Chemistry*, 2011, **2011**, 4985-4992.
56 V. N. Dorofeeva, S. V. Kolotilov, M. A. Kiskin, R. A. Polunin, Z. V. Dobrokhotova, O. Cador, S. Golhen, L. Ouahab, I. L. Eremenko, V. M. Novotortsev, *Chemistry – A European Journal*, 2012, **18**, 5006-5012.
57 R. A. Polunin, M. A. Kiskin, O. Cador, S. V. Kolotilov, *Inorganica Chimica Acta*, 2012, **380**, 201-210.
58 G. Ferey, *Chemical Society Reviews*, 2008, **37**, 191-214.
59 S. Surblé, C. Serre, C. Mellot-Draznieks, F. Millange, G. Férey, *Chemical Communications*, 2006, 284.
60 C. Mellot-Draznieks, C. Serre, S. Surblé, N. Audebrand, G. Férey, *Journal of the American Chemical Society*, 2005, **127**, 16273-16278.
61 C. Serre, C. Mellot-Draznieks, S. Surblé, N. Audebrand, Y. Filinchuk, G. Férey, *Science*, 2007, **315**, 1828-1831.
62 C. Serre, F. Millange, C. Thouvenot, M. Noguès, G. Marsolier, D. Louër, G. Férey, *Journal of the American Chemical Society*, 2002, **124**, 13519-13526; S. Kitagawa, K. Uemura, *Chemical Society Reviews*, 2005, **34**, 109-119.
63 S. Bauer, C. Serre, T. Devic, P. Horcajada, J. Marrot, G. Férey, N. Stock, *Inorganic Chemistry*, 2008, **47**, 7568-7576.
64 S. Ma, J. M. Simmons, D. Yuan, J.-R. Li, W. Weng, D.-J. Liu, H.-C. Zhou, *Chemical Communications*, 2009, 4049-4051.
65 J. P. S. Mowat, S. R. Miller, A. M. Z. Slawin, V. R. Seymour, S. E. Ashbrook, P. A. Wright, *Microporous and Mesoporous Materials*, 2011, **142**, 322-333.
66 F. Carson, J. Su, A. E. Platero-Prats, W. Wan, Y. Yun, L. Samain, X. Zou, *Crystal Growth & Design*, 2013, **13**, 5036-5044.
67 P. Horcajada, F. Salles, S. Wuttke, T. Devic, D. Heurtaux, G. Maurin, A. Vimont, M. Daturi, O. David, E. Magnier, N. Stock, Y. Filinchuk, D. Popov, C. Riekel, G. Férey, C. Serre, *Journal of the American Chemical Society*, 2011, **133**, 17839-17847.
68 M. Dan-Hardi, H. Chevreau, T. Devic, P. Horcajada, G. Maurin, G. Férey, D. Popov, C. Riekel, S. Wuttke, J.-C. Lavalley, A. Vimont, T. Boudewijns, D. de Vos, C. Serre, *Chemistry of Materials*, 2012, **24**, 2486-2492.
69 M. O'Keeffe, *Materials Research Bulletin*, 2006, **41**, 911-915.
70 M. Latroche, S. Surblé, C. Serre, C. Mellot-Draznieks, P. L. Llewellyn, J.-H. Lee, J.-S. Chang, S. H. Jhung, G. Férey, *Angewandte Chemie International Edition*, 2006, **45**, 8227-8231.
71 E. Soubeyrand-Lenoir, C. Vagner, J. W. Yoon, P. Bazin, F. Ragon, Y. K. Hwang, C. Serre, J.-S. Chang, P. L. Llewellyn, *Journal of the American Chemical Society*, 2012, 10174-10181.
72 P. L. Llewellyn, S. Bourrelly, C. Serre, A. Vimont, M. Daturi, L. Hamon, G. De Weireld, J.-S. Chang, D.-Y. Hong, Y. Kyu Hwang, S. Hwa Jhung, G. Férey, *Langmuir*, 2008, **24**, 7245-7250.
73 P. Horcajada, C. Serre, M. Vallet-Regí, M. Sebban, F. Taulelle, G. Férey, *Angewandte Chemie International Edition*, 2006, **45**, 5974-5978; P. Horcajada, T. Chalati, C. Serre, B. Gillet, C. Sebrie, T. Baati, J. F. Eubank, D. Heurtaux, P. Clayette, C. Kreuz, J.-S. Chang, Y. K. Hwang, V. Marsaud, P.-N. Bories, L. Cynober, S. Gil, G. Férey, P. Couvreur, R. Gref, *Nat Mater*, 2010, **9**, 172-178; D. Cunha, M. Ben Yahia, S. Hall, S. R. Miller, H. Chevreau, E. Elkaïm, G. Maurin, P. Horcajada, C. Serre, *Chemistry of Materials*, 2013, **25**, 2767-2776.
74 K. M. L. Taylor-Pashow, J. D. Rocca, Z. Xie, S. Tran, W. Lin, *Journal of the American Chemical Society*, 2009, **131**, 14261-14263.
75 P. Horcajada, S. Surbl, C. Serre, D.-Y. Hong, Y.-K. Seo, J.-S. Chang, J.-M. Grenoche, I. Margiolaki, G. Férey, *Chemical Communications*, 2007, 2820.
76 P. Serra-Crespo, E. V. Ramos-Fernandez, J. Gascon, F. Kapteijn, *Chemistry of Materials*, 2011, **23**, 2565-2572.
77 L. Hamon, C. Serre, T. Devic, T. Loiseau, F. Millange, G. r. Férey, G. D. Weireld, *Journal of the American Chemical Society*, 2009, **131**, 8775-8777.
78 J. W. Yoon, Y.-K. Seo, Y. K. Hwang, J.-S. Chang, H. Leclerc, S. Wuttke, P. Bazin, A. Vimont, M. Daturi, E. Bloch, P. L. Llewellyn, C. Serre, P. Horcajada, J.-M. Grenèche, A. E. Rodrigues, G. Férey, *Angewandte Chemie International Edition*, 2010, **49**, 5949-5952.
79 S. Biswas, S. Couck, M. Grzywa, J. F. M. Denayer, D. Volkmer, P. Van Der Voort, *European Journal of Inorganic Chemistry*, 2012, 2481-2486.
80 A. Sonnauer, F. Hoffmann, M. Fröba, L. Kienle, V. Duppel, M. Thommes, C. Serre, G. Férey, N. Stock, *Angewandte Chemie International Edition*, 2009, **48**, 3791-3794.
81 M. Lammert, S. Bernt, F. Vermoortele, D. E. De Vos, N. Stock, *Inorganic Chemistry*, 2013, **52**, 8521-8528.
82 S. Bernt, V. Guillerm, C. Serre, N. Stock, *Chemical Communications*, 2011, **47**, 2838-2840.
83 M. G. Goesten, J. Juan-Alcañiz, E. V. Ramos-Fernandez, K. B. Sai Sankar Gupta, E. Stavitski, H. van Bekkum, J. Gascon, F. Kapteijn, *Journal of Catalysis*, 2011, **281**, 177-187.
84 Y. K. Hwang, D.-Y. Hong, J.-S. Chang, S. H. Jhung, Y.-K. Seo, J. Kim, A. Vimont, M. Daturi, C. Serre, G. Férey, *Angewandte Chemie International Edition*, 2008, **47**, 4144-4148; M. Banerjee, S. Das, M. Yoon, H. J. Choi, M. H. Hyun, S. M. Park, G. Seo, K. Kim, *Journal of the American Chemical Society*, 2009, **131**, 7524-7525.

85 G. Férey, C. Mellot-Draznieks, C. Serre, F. Millange, *Accounts of Chemical Research*, 2005, **38**, 217-225.
86 C. Mellot-Draznieks, J. Dutour, G. Férey, *Zeitschrift für anorganische und allgemeine Chemie*, 2004, **630**, 2599-2604.
87 D. Yuan, R. B. Getman, Z. Wei, R. Q. Snurr, H.-C. Zhou, *Chemical Communications*, 2012, **48**, 3297-3299.
88 H. Chevreau, T. Devic, F. Salles, G. Maurin, N. Stock, C. Serre, *Angewandte Chemie International Edition*, 2013, **52**, 5056-5060.
89 K. Koh, A. G. Wong-Foy, A. J. Matzger, *Angewandte Chemie International Edition*, 2008, **47**, 677-680; K. Koh, A. G. Wong-Foy, A. J. Matzger, *Journal of the American Chemical Society*, 2009, **131**, 4184-4185; K. Koh, A. G. Wong-Foy, A. J. Matzger, *Journal of the American Chemical Society*, 2010, **132**, 15005-15010; H. Furukawa, N. Ko, Y. B. Go, N. Aratani, S. B. Choi, E. Choi, A. Ö. Yazaydin, R. Q. Snurr, M. O'Keeffe, J. Kim, O. M. Yaghi, *Science*, 2010, **329**, 424-428.
90 Y. Liu, J. F. Eubank, A. J. Cairns, J. Eckert, V. C. Kravtsov, R. Luebke, M. Eddaoudi, *Angewandte Chemie International Edition*, 2007, **46**, 3278-3283.
91 D. N. Dybtsev, H. Chun, K. Kim, *Angewandte Chemie International Edition*, 2004, **43**, 5033-5036; K. Uemura, Y. Yamasaki, Y. Komagawa, K. Tanaka, H. Kita, *Angewandte Chemie International Edition*, 2007, **46**, 6662-6665; O. K. Farha, C. D. Malliakas, M. G. Kanatzidis, J. T. Hupp, *Journal of the American Chemical Society*, 2009, **132**, 950-952.
92 Y.-B. Zhang, W.-X. Zhang, F.-Y. Feng, J.-P. Zhang, X.-M. Chen, *Angewandte Chemie International Edition*, 2009, **48**, 5287-5290.
93 Y.-B. Zhang, H.-L. Zhou, R.-B. Lin, C. Zhang, J.-B. Lin, J.-P. Zhang, X.-M. Chen, *Nature Communications*, 2012, **3**, 642.
94 G. Jiang, T. Wu, S.-T. Zheng, X. Zhao, Q. Lin, X. Bu, P. Feng, *Crystal Growth & Design*, 2011, **11**, 3713-3716; E. Yang, Z.-S. Liu, S. Lin, S.-Y. Chen, *Inorganic Chemistry Communications*, 2011, **14**, 1588-1590.
95 J. Jia, X. Lin, C. Wilson, A. J. Blake, N. R. Champness, P. Hubberstey, G. Walker, E. J. Cussen, M. Schroder, *Chemical Communications*, 2007, 840-842.
96 X.-M. Zhang, Y.-Z. Zheng, C.-R. Li, W.-X. Zhang, X.-M. Chen, *Crystal Growth & Design*, 2007, **7**, 980-983.
97 Y.-S. Wei, K.-J. Chen, P.-Q. Liao, B.-Y. Zhu, R.-B. Lin, H.-L. Zhou, B.-Y. Wang, W. Xue, J.-P. Zhang, X.-M. Chen, *Chemical Science*, 2013, **4**, 1539-1546.
98 Q. Zhai, Q. Lin, T. Wu, S.-T. Zheng, X. Bu, P. Feng, *Dalton Transactions*, 2012, **41**, 2866-2868.
99 J. Zhang, S. Chen, X. Bu, *Angewandte Chemie International Edition*, 2008, **47**, 5434-5437; S. Chen, J. Zhang, T. Wu, P. Feng, X. Bu, *Journal of the American Chemical Society*, 2009, **131**, 16027-16029.
100 C. Volkringer, T. Loiseau, *Materials Research Bulletin*, 2006, **41**, 948-954.
101 S.-T. Zheng, J. T. Bu, Y. Li, T. Wu, F. Zuo, P. Feng, X. Bu, *Journal of the American Chemical Society*, 2010, **132**, 17062-17064.
102 S.-T. Zheng, T. Wu, F. Zuo, C. Chou, P. Feng, X. Bu, *Journal of the American Chemical Society*, 2012, **134**, 1934-1937.
103 S.-T. Zheng, J. J. Bu, T. Wu, C. Chou, P. Feng, X. Bu, *Angewandte Chemie International Edition*, 2011, **50**, 8858-8862; X. Gu, Z.-H. Lu, Q. Xu, *Chemical Communications*, 2010, **46**, 7400-7402.
104 J. Jia, F. Sun, T. Borjigin, H. Ren, T. Zhang, Z. Bian, L. Gao, G. Zhu, *Chemical Communications*, 2012, **48**, 6010-6012.
105 S.-T. Zheng, X. Zhao, S. Lau, A. Fuhr, P. Feng, X. Bu, *Journal of the American Chemical Society*, 2013, **135**, 10270-10273.
106 A. Schoedel, L. Wojtas, S. P. Kelley, R. D. Rogers, M. Eddaoudi, M. J. Zaworotko, *Angewandte Chemie International Edition*, 2011, **50**, 11421-11424.
107 V. D. Vreshch, A. B. Lysenko, A. N. Chernega, J. A. K. Howard, H. Krautscheid, J. Sieler, K. V. Domasevitch, *Dalton Transactions*, 2004, 2899-2903; J. M. Ellsworth, H.-C. zur Loye, *Dalton Transactions*, 2008, 5823; L. Carlucci, G. Ciani, S. Maggini, D. M. Proserpio, M. Visconti, *Chemistry - A European Journal*, 2010, **16**, 12328-12341.
108 A. Schoedel, L. Wojtas, M. Zaworotko, *unpublished results*.
109 E. Gonzalez-Vergara, J. Hegenauer, P. Saltman, *Inorganica Chimica Acta*, 1982, **66**, 115-118.
110 T. Li, M. T. Kozlowski, E. A. Doud, M. N. Blakely, N. L. Rosi, *Journal of the American Chemical Society*, 2013, **135**, 11688-11691; H. Deng, S. Grunder, K. E. Cordova, C. Valente, H. Furukawa, M. Hmadeh, F. Gándara, A. C. Whalley, Z. Liu, S. Asahina, H. Kazumori, M. O'Keeffe, O. Terasaki, J. F. Stoddart, O. M. Yaghi, *Science*, 2012, **336**, 1018-1023.
111 S. K. Elsaidi, M. H. Mohamed, L. Wojtas, A. J. Cairns, M. Eddaoudi, M. J. Zaworotko, *Chemical Communications*, 2013, **49**, 8154-8156.
112 A. Schoedel, A. J. Cairns, Y. Belmabkhout, L. Wojtas, M. Mohamed, Z. Zhang, D. M. Proserpio, M. Eddaoudi, M. J. Zaworotko, *Angewandte Chemie International Edition*, 2013, **52**, 2902-2905.
113 K. A. Cychosz, A. J. Matzger, *Langmuir*, 2010, **26**, 17198-17202; K. Koh, J. D. Van Oosterhout, S. Roy, A. G. Wong-Foy, A. J. Matzger, *Chemical Science*, 2012, **3**, 2429-2432.
114 S. A. Bourne, J. Lu, A. Mondal, B. Moulton, M. J. Zaworotko, *Angewandte Chemie International Edition*, 2001, **40**, 2111-2113.
115 A. Schoedel, W. Boyette, L. Wojtas, M. Eddaoudi, M. J. Zaworotko, *Journal of the American Chemical Society*, 2013.
116 F. Allen, *Acta Crystallographica Section B*, 2002, **58**, 380-388.
117 N. C. Burtch, H. Jasuja, D. Dubbeldam, K. S. Walton, *Journal of the American Chemical Society*, 2013, **135**, 7172-7180.
118 S. Ma, D. Sun, J. M. Simmons, C. D. Collier, D. Yuan, H.-C. Zhou, *Journal of the American Chemical Society*, 2008, **130**, 1012-1016; Y. Peng, V. Krungleviciute, I. Eryazici, J. T. Hupp, O. K. Farha, T. Yildirim, *Journal of the American Chemical Society*, 2013, **135**, 11887-11894.